Journal of Virology, Mar. 2009, p. 2075–2087 Vol. 83, No. 5
0022-538X/09/$08.00+0 doi:10.1128/JVI.02007-08

Host Responses to Wild-Type and Attenuated Herpes Simplex Virus Infection in the Absence of Stat1 ▽ ‡

Tracy Jo Pasieka,[1]† Cristian Cilloniz,[2,3]† Betty Lu,[1] Thomas H. Teal,[2,3] Sean C. Proll,[2,3] Michael G. Katze,[2,3] and David A. Leib[1,4]*

Departments of Ophthalmology and Visual Sciences[1] and Molecular Microbiology,[4] Washington University School of Medicine, St. Louis, Missouri 63110, and Department of Microbiology, University of Washington School of Medicine,[2] and Washington National Primate Research Center,[3] Seattle, Washington 98195

Received 23 September 2008/Accepted 12 December 2008

Humans and mice lacking the interferon signaling molecule Stat1 are sensitive to a variety of pathogens due to their presumed inability to mount a strong innate immune response. The herpes simplex virus type 1 (HSV-1) virion host shutoff (vhs) protein is a multifunctional immunomodulator that counteracts the innate immune response and viruses lacking vhs are attenuated and effective live vaccines in animal models. To investigate the interplay of viruses with an immunocompromised host, we performed functional genomics analyses on control and Stat1$^{-/-}$ mouse corneas infected with wild-type or vhs-null viruses. In control mice, correlative with viral growth, both viruses induced a transient increase in immunomodulators, followed by viral clearance. In contrast, infection of the Stat1$^{-/-}$ mice induced a heightened and prolonged induction of inflammatory modulators for both viruses, manifesting as a significant immune cell infiltrate and ocular disease. Moreover, while wild-type virus infection of Stat1$^{-/-}$ was always lethal, vhs-null infection was rarely lethal. There was a significant increase in Stat3- and interleukin-6 (IL-6)-dependent transcription in Stat1$^{-/-}$ mice, implicating the Stat3 and IL-6 pathways in the observed ocular pathology. Further, infected Stat1$^{-/-}$ mice showed phosphorylated Stat3 in the corneal epithelium. Our data show a role for vhs in evading innate host responses and a role for Stat1 in limiting virus infection and for facilitating an appropriate nonpathological inflammatory response.

The innate immune response and the rapid establishment of an antiviral state are critical determinants for the control of viral infections. Loss or deletion of such pathways often results in severe disease after infection with otherwise benign and ubiquitous pathogens, both in humans and in experimental animals (10, 17). For their part, viruses have evolved a variety of strategies to counter specific aspects of innate immunity, and viruses lacking genes or *cis*-acting elements responsible for the countering of innate immunity are highly attenuated (39).

Herpes simplex virus (HSV) exhibits two distinct phases of infection. Acute infection occurs at peripheral mucocutaneous sites such as the cornea and skin and involves the expression of all classes of viral genes. Latency is established in innervating neurons and is characterized by limited gene expression and persistence of viral nucleic acids within neuronal nuclei. Periodic reactivation may result in shedding of infectious virus back to the site of infection and associated an severe corneal disease known as herpetic stromal keratitis (HSK) (reviewed in reference 47). HSK consists of immunopathological inflammation, loss of visual acuity, and even blindness. It has therefore been well studied in humans and animal models. Recognition of HSV-1 infection in vivo is thought to be mediated by Toll-like receptors (TLRs) expressed on corneal epithelial cells (16, 40). Once viral infection is recognized, TLR2 and TLR9 activation (20, 26) initiates a cascade of signaling events leading to the expression of numerous immune modulators that increase inflammation and immune cell activities (3, 7). This cascade plays a role in inducing HSK (reviewed in reference 7).

In common with many pathogens, HSV-1 has genes to manipulate the host cell environment during acute infection to ensure a successful viral life cycle (23). These include the virion host shutoff protein (vhs), the product of the UL41 gene, which is highly conserved among the neurotropic herpesviruses (23). vhs is present in the tegument of virions and it is synthesized with leaky-late kinetics. It has RNase activity and degrades both cellular and viral mRNA (21), with little or no effect on rRNA or tRNA. Although dispensable for viral replication in vitro, vhs has a pivotal role in pathogenesis since HSV-1 vhs-null viruses are severely attenuated in mouse models (43). vhs-null viruses are also effective as live-attenuated vaccines in experimental mouse models (19, 29, 48, 49). vhs plays a role in the evasion of the host innate immune response, as supported by several studies. Growth of an HSV-1 vhs-null virus is severely attenuated in both wild-type and gamma interferon (IFN-γ) receptor-deficient (IFNγR$^{-/-}$) mice but partially restored in IFN$\alpha\beta$R$^{-/-}$ and IFN$\alpha\beta\gamma$R$^{-/-}$ mice following corneal inoculation (24). Similarly, growth of an HSV-2 vhs-null virus was almost completely restored in IFN-α/$\beta^{-/-}$ mice (30). We recently reported that this virus is hypersensitive to IFN pretreatment in mouse embryo fibroblasts (MEFs) and that growth of this virus is restored to near wild-type virus levels in IFN$\alpha\beta\gamma$R$^{-/-}$ MEFs (32). Furthermore, enhanced proinflam-

* Corresponding author. Mailing address: Washington University School of Medicine, Department of Ophthalmology and Visual Sciences, 660 South Euclid Ave., Box 8096, St. Louis, MO 63110. Phone: (314) 362-2689. Fax: (314) 362-3638. E-mail: leib@vision.wustl.edu.

† T.J.P. and C.C. contributed equally to this study.

‡ Supplemental material for this article may be found at http://jvi.asm.org/.

▽ Published ahead of print on 24 December 2008.

matory cytokine production (interleukin-1β [IL-1β], IL-8, and macrophage inflammatory protein 1α [MIP-1α]) was noted in three different human cell lines infected with a *vhs*-null virus (44).

We examined the replication, pathogenesis, and functional genomics of wild-type (WT) and *vhs*-deficient (Δ*vhs*) virus infection of the corneas of control and Stat1-deficient mice. Stat1 (for signal transducer and activator of transcription 1) is a transcription factor critical for transmitting the signal from the IFN receptor to initiate the upregulation of IFN-stimulated genes (ISGs), a subset of genes stimulated through recognition of type 1 and type II IFNs. Stat1$^{-/-}$ mice are highly susceptible to a variety of infections, including *Listeria monocytogenes*, vesicular stomatitis virus, and mouse cytomegalovirus (MCMV) infections (13, 27). Consistent with these observations, the corneas of Stat1$^{-/-}$ mice following infection with both WT and Δ*vhs* viruses exhibited increased viral replication and pathology compared to control mice. Unexpectedly, our data showed increased expression of a variety of IFN-induced genes and a related increase in inflammation and pathology in Stat1$^{-/-}$ mice, which indicates that the presence of Stat1is important for mounting an appropriate, nonpathological inflammatory response. Our data also demonstrated that vhs plays a fundamental role in promoting viral replication, since the Δ*vhs* virus remained attenuated in the absence of Stat1.

MATERIALS AND METHODS

Cells, viruses, and mice. Vero cells were used for amplification and the determination of viral stock titers as previously described (35). The HSV-1 wild-type strain KOS was the background for all viruses in the present study (42). Construction of the *vhs*-null virus HSV-1 (Δ*vhs*) virus has been described (43). Mock-treated animals were inoculated with uninfected Vero cell lysates prepared in a manner parallel to that for infected Vero lysates. The mouse strains used were the control 129S6 as WT mice (Taconic Farms, Germantown, NY) and 129 S6 Stat1 knockout mice (Stat1$^{-/-}$) (27). Mice were housed in the Washington University School of Medicine enhanced barrier facility and infected in the Washington University School of Medicine biohazard facility. At both facilities, sentinel mice were screened every 3 months and determined to be negative for adventitious mouse pathogens, in particular mouse norovirus. Mice were infected at between 6 and 8 weeks of age. Mice were euthanized when necessary in accordance with all federal and university policies.

Animal infection procedures. For corneal infection, equal numbers of male and female mice were anesthetized intraperitoneally with ketamine (87 mg/kg of body weight) and xylazine (13 mg/kg). Corneas were bilaterally scarified with a 25G syringe needle, and virus was inoculated by adding 2×10^6 PFU in a 5-μl volume. Mice were sacrificed at the specified time postinfection, and eye swab material was collected for a standard plaque assay as previously described (35). Titers were derived from at least 20 animals and collected from four independent groups of mice. The amount of virus is reported as PFU per milliliter of swab material from each cornea.

Disease scoring of infected animals. Mice were infected using the corneal inoculation procedure described above. At the indicated time postinfection, mice were weighed and observed for disease pathology and evaluated using the following disease scores: 0, no visible lesions; 1, minimal eyelid swelling; 2, moderate eyelid swelling and crusty ocular discharge; 3, severe eyelid swelling, moderate periocular hair loss, and skin lesions; and 4, severe eyelid swelling with eyes crusted shut, severe periocular hair loss, and skin lesions. Mice were scored individually, and the reported disease score was determined by averaging the disease score for the infection group. Changes in body weight are reported as the percent weight change from day 1 postinfection. Disease scores were measured from at least 20 mice, with the exception of later time points, by which time some mice had succumbed to infection.

Harvest of cornea total RNA for DNA microarray analysis. For each time point and infection condition, the corneas of five mice of mixed genders were pooled for microarray analysis. At the indicated time postinfection, corneas were removed, rinsed in phosphate-buffered saline, cleaned of extraneous tissue, placed in 0.3 ml of solution D (4 M guanidine thiocyanate, 25 ml of sodium citrate, 0.5% sarcosyl, 0.1 M 2-mercaptoethanol) (8), and stored at −80°C. Total RNA was harvested from homogenized tissue as previously described (31). RNA quality was evaluated by using an Agilent 2100 bioanalyzer (Agilent Technologies, Palo Alto, CA). Total RNA was amplified and labeled by using a Low RNA Input Linear Amp kit (Agilent).

Oligonucleotide microarray analysis. Microarray protocols and analysis have been described previously (31). Briefly, probes were hybridized on Agilent mouse oligonucleotide microarray slides (approximately 20,000 unique mouse genes). Each single microarray experiment incorporated reverse dye labeling techniques and resulted in two measurements for each gene ($n = 2$), allowing the calculation of a mean ratio between expression levels, standard deviations, and *P* values within the Rosetta resolver system (Rosetta Biosoftware, Seattle, WA). Slides were scanned with an Agilent DNA microarray scanner, and image data was processed by using an Agilent feature extractor (Agilent). Before the data are uploaded into a Rosetta Resolver 6.0, the Agilent system performs error modeling. The data were entered into a custom-design database (Expression Array Manager) and uploaded into Rosetta Resolver 6.0, which generates expression data such as *P* values and error measurements. The Resolver system performs a squeeze operation that creates ratio profiles by combining replicates while applying error weighting. The error weighting consists of adjusting for additive and multiplicative noise. A *P* value is generated that represents the probability that a gene is differentially expressed. In the present study, a threshold *P* value of 0.01 was used to identify genes that were significantly differentially expressed. The Resolver system then combines ratio profiles to create ratio experiments using an error-weighted average as described by Stoughton and Dai (42a). Spotfire Decision Site 8.1 (Spotfire, Somerville, MA), and Ingenuity Pathway Analysis (IPA; Ingenuity Systems) were also utilized for data analysis and mining. Microarray format, protocols, and data can be viewed at http://expression.viromics.washington.edu.

Bio-Plex cytokine analysis. Corneas were isolated and lysed in a cell lysis kit (Bio-Rad, Hercules, CA) in accordance with the kit protocol. Both corneas from one mouse were combined to form one sample. Briefly, corneas were rinsed, lysed in a 100-μl volume, homogenized, sonicated, and then centrifuged at 4.5 × *g* for 4 min to remove debris. Equivalent amounts of protein, as measured by Bradford assay, were added to each Bio-Plex well of a multiplex mouse cytokine Bio-Plex array. Cytokine concentrations are reported as pg/ml. The results shown are the average from two experiments, with each experiment containing two or more mice per data point ($n \geq 4$). The *P* value was determined by using a two-tailed, unpaired *t* test. As performed for the genomics analysis, the $\log_2$ ratio (infected to uninfected) of the averaged pg/ml was calculated.

Western blot analysis. At the indicated times postinfection, corneas were isolated, lysed, and homogenized in 200 μl of 2× lysis buffer containing 10% β-mercaptoethanol. Samples consisting of both corneas from one mouse were loaded onto a 10% polyacrylamide electrophoresis gel and transferred to polyvinylidene difluoride membranes that were then cut for separate probing of Stat3 and actin. Secondary antibody incubation was followed by detection with an ECL Plus Western blotting detection kit (Amersham Biosciences, England). Images were collected with a Molecular Dynamics Storm 860 phosphorimaging system. Band analysis was performed with ImageQuant TL. The antibodies used were as follows: beta-actin (Sigma), Stat3 (catalog no. 9132; Cell Signaling Technology, Danvers, MA) p-Stat3 Y705 (sc-7993; Santa Cruz), and goat anti-mouse and goat anti-rabbit horseradish peroxidase (HRP) conjugates (Bio-Rad).

Immunohistochemistry. At the indicated day postinfection, eyeballs from two mice per infection condition and time point ($n = 4$) were enucleated and immediately fixed in 10% buffered neutral formalin. Paraffin-embedded sections of 4 μm were stained with hematoxylin to identify nuclei. Primary antibodies were detected with streptavidin-HRP and DAB. Primary antibodies used included anti-Ly-6G and Ly-6C (Gr-1) antibody (BD Pharmingen, San Diego, CA) and anti-phospho-Stat3 Y705 (D3A7 #9145; Cell Signaling Technology). Sections were imaged at a ×40 magnification.

RESULTS

Acute replication of HSV-1 is significantly enhanced in the corneas of Stat1$^{-/-}$ mice. To examine the role of the innate response in controlling WT and an attenuated virus (Δ*vhs* virus) replication, we inoculated the corneas of control mice and mice lacking the IFN signaling factor Stat1 (27). In the corneas of control mice, WT virus was readily detected in corneas out to 6 days postinfection (dpi) (Fig. 1A), while the

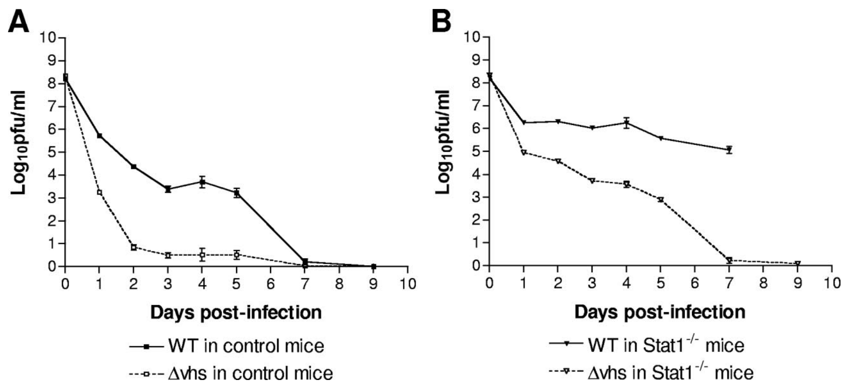

FIG. 1. Acute replication of HSV-1 in corneas. Corneas of control and Stat1$^{-/-}$ mice were scarified and inoculated with 2×10^6 PFU/eye of either WT virus (A) or Δ*vhs* virus (B). Eye swabs were taken at indicated times postinfection, and titers were determined on Vero cells. Each data point represents eye swab titers from at least 20 mice in four separate experiments.

Δ*vhs* virus was rapidly cleared and fell to minimally detectable levels within 2 dpi. In the corneas of the Stat1$^{-/-}$ mice, WT virus showed a significant and prolonged increase in growth compared to the control mice (Fig. 1B). In contrast to its phenotype in control mice, Δ*vhs* virus in the Stat1$^{-/-}$ mice replicated to high levels, comparable to those of the WT virus in the control mice. The enhanced growth of both viruses in the Stat1$^{-/-}$ mice and the attenuation of the Δ*vhs* virus in both mouse strains indicated Stat1- and vhs-dependent mechanisms in controlling viral growth.

Disease and pathology is significantly enhanced in corneas of Stat1$^{-/-}$ mice. We further characterized HSV-1 pathogenesis by observing corneal disease pathology and changes in body weight during the course of infection (Fig. 2). In control mice, WT virus infection resulted in a mild ocular disease, consisting of eyelid swelling and minimal ocular discharge, while Δ*vhs* virus infection caused little if any disease (Fig. 2A and B). Furthermore, control mice infected with WT or Δ*vhs* virus did not exhibit any significant weight change. In contrast, WT virus infection of the Stat1$^{-/-}$ mice caused severe ocular disease that rapidly progressed to periocular hair loss, skin lesions, dramatic weight loss, and death (Fig. 2C). These mice showed symptoms of encephalitis (hind limb paralysis, labored breathing, lack of movement) with more than 90% of the mice dying within 7 days. HSV-1 Δ*vhs* infection of the Stat1$^{-/-}$ mice also induced substantial disease pathology, weight loss, and similar symptoms of encephalitis, with <5% death (Fig. 2D). Of interest, WT virus- and Δ*vhs* virus-infected Stat1$^{-/-}$ mice were similar in that both demonstrated substantial corneal opacity and discharge by 2 dpi. Between 5 and 7 dpi, the disease in these mice differentiated, as the Δ*vhs* virus-infected Stat1$^{-/-}$ mice showed improvement in terms of corneal opacity and disease pathology.

An analysis of brain titers between 3 and 9 dpi revealed a close correlation between symptoms of encephalitis and virus titers (33). In the brains of control mice, WT virus was only transiently detectable, while Δ*vhs* virus was undetectable. In contrast, in the brains of Stat1$^{-/-}$ mice, both WT and Δ*vhs* viruses were detected, with the WT virus at elevated titers throughout the time course and the Δ*vhs* virus cleared by 7 dpi. Overall, the trigeminal ganglia, periocular skin, and brain titers closely resembled the pattern observed for cornea replication. It is of interest that the Stat1$^{-/-}$ mice, while displaying substantial disease pathology, still cleared Δ*vhs* virus infection.

Corneal histology shows neutrophil invasion of Stat1$^{-/-}$ corneas. Corneal inflammation is an interleukin-6 (IL-6)-mediated process with rapid infiltration of neutrophils and thickening of the stromal layer (12). Neutrophils are the first cells to enter the cornea following HSV-1 infection, and infiltration peaks at 2 dpi (46). The corneal opacity found in the infected Stat1$^{-/-}$ mice prompted us to examine immune cell infiltration and pathology in the corneas of these mice via immunohistochemistry. Sections of mock-treated and virus-infected corneas at 3 dpi were sectioned and labeled with Ly-6G/Ly-6C to identify neutrophils.

Control and Stat1$^{-/-}$ mock treated mice showed an intact epithelial cell layer and stroma devoid of neutrophils (Fig. 3A and D). Striking differences were observed, however, between the infected control and Stat1$^{-/-}$ mice. The WT virus-infected control mouse corneas showed some evidence of thinning epithelial layer, but few Ly-6^{+} cells in the stroma, while the Δ*vhs* virus-infected control corneas closely resembled the mock-treated corneas (Fig. 3B and C). In contrast, both the WT virus- and the Δ*vhs* virus-infected Stat1$^{-/-}$ mice showed extensive loss of the corneal epithelial layer, a thickening of the stromal layer, and numerous Ly-6^{+} infiltrating cells (Fig. 3E and F). It is notable that while the degree of inflammation and damage for each infection condition correlated closely with the disease scores and corneal opacity observed in the Stat1$^{-/-}$ mice (Fig. 2), it did not correlate with viral replication. The replication of WT virus in control mice was comparable to that of Δ*vhs* in Stat1$^{-/-}$ mice, and yet the patterns of inflammation and damage were distinct.

Overview of transcriptional profiling experimental design and analysis. Our analyses thus far suggest a role for vhs in promoting viral replication and a role for Stat1 in controlling the initial response to viral infection. These observations raised two questions. First, how does the absence of Stat1 impact the host response? Second, how does host gene expression differ under circumstances in which the growth of the WT and Δ*vhs* viruses was equivalent? The latter question addresses the assumption that gene expression correlates with viral replication. Because differences in viral growth were observed in the first

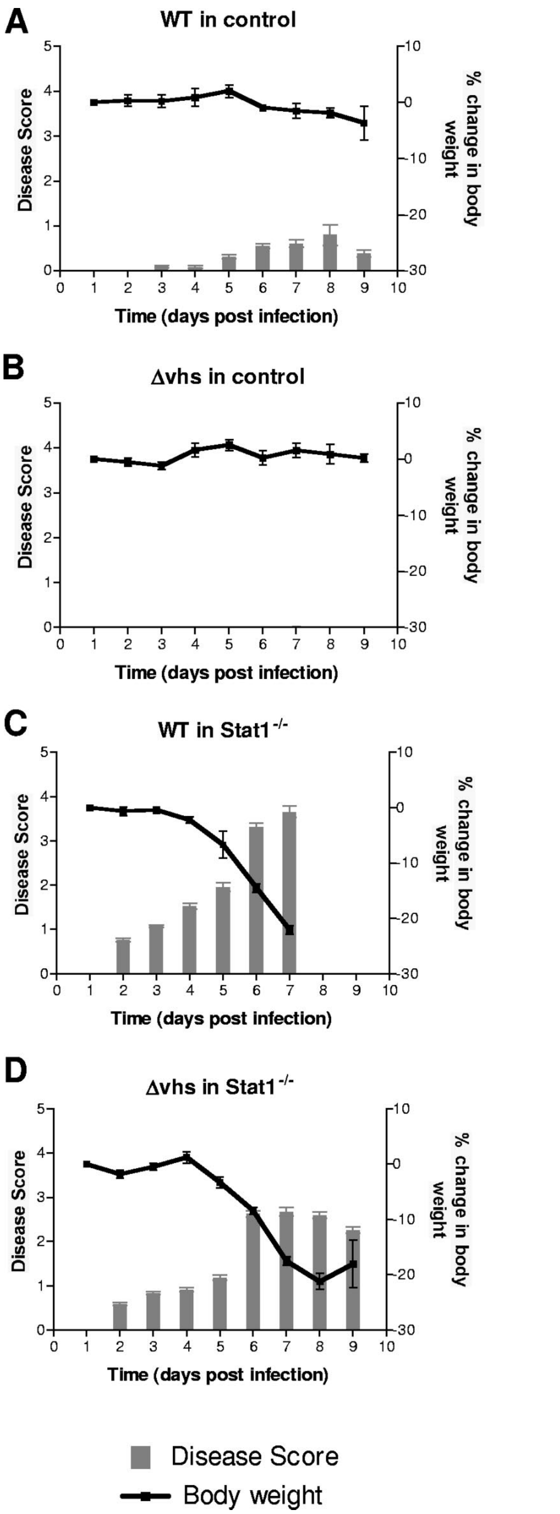

FIG. 2. Pathology following HSV-1 infection. Corneas of control and Stat1$^{-/-}$ mice were scarified and inoculated with 2×10^6 PFU/eye. Periocular disease score (gray bars) and weight changes (black lines) were recorded. Disease score parameters are detailed in Materials and Methods. Weight changed in grams was measured on indicated days postinfection. Each data point represents the disease score and weight change from at least 20 mice in four separate experiments.

few days postinfection, we focused our gene expression analysis on cornea tissue over the first 3 dpi.

To address these questions, the corneas of control mice or Stat1$^{-/-}$ mice were inoculated with a lysate of mock-infected Vero cells, WT virus, or Δ*vhs* virus. Total RNA was harvested, processed, and hybridized to Agilent mouse DNA microarrays. For each infection condition and time point, one sample of pooled RNA was hybridized twice (dye-flip) to generate an $n = 2$ for each gene. All gene expression changes for infected cells are presented as a fold change compared to a mouse- and time-matched mock infection. Only genes that changed ≥2-fold compared to mock-infected cells ($P \leq 0.01$) in at least one of the six infection conditions for each virus were considered for further analysis.

Genes that met our selection parameters were organized into heat maps to show patterns of gene expression changes due to WT virus (Fig. 4A) and Δ*vhs* virus (Fig. 4B) infection. For both viruses in either mouse strain, most gene expression changes reflected the host's initial response to infection, with the most prominent transcriptional changes involving IFN-, IL-6-, and TLR-dependent genes. Although the types of genes changed were similar in each infection, the overall number and magnitude of these changes were more pronounced in the Stat1$^{-/-}$ mice, suggesting either a Stat1- or viral replication-dependent effect. For the WT virus in the control mouse, the peak number of changed genes was 599 at 2 dpi, while in the Stat1$^{-/-}$ mouse the peak number was 1864 also at 2 dpi. For the Δ*vhs* virus in the control mouse, the peak number was 351 genes at 2 dpi, while the peak in the Stat1$^{-/-}$ mice was 1,154 genes at 3 dpi.

In either mouse strain, Δ*vhs* virus-infected mice exhibited fewer gene expression changes, suggesting that the host response can reflect the level of viral growth. Stat1$^{-/-}$ mice exhibited increased inflammatory gene expression, in terms of both number of induced genes, as well as magnitude of induction. Also, Stat1$^{-/-}$ mice exhibited a temporal delay of ISG and inflammatory gene expression, in that many genes upregulated by 1 dpi in the control mice were not upregulated in the Stat1$^{-/-}$ until 2 or 3 dpi. This suggested that Stat1-independent IFN signaling took longer to initiate in Stat1$^{-/-}$ mice, perhaps allowing the virus to gain an advantage over the host.

Unexpectedly, when all four infection models were compared, we found that the level of viral replication did not correlate with the number and magnitude of gene expression changes. This idea is exemplified by comparing the hierarchy of replication at 2 dpi (Stat1$^{-/-}$/WT > control/WT = Stat1$^{-/-}$/Δ*vhs* > control/Δ*vhs*) to the hierarchy of the number of changed genes on the same day (Stat1$^{-/-}$/WT > Stat1$^{-/-}$/Δ*vhs* > control/WT > control/Δ*vhs*). Rather, we found that the presence or absence of vhs had a greater effect on viral replication, while the presence or absence of Stat1 had a greater effect on the host transcriptional response to infection and disease pathology. This unanticipated observation demonstrated a lack of correlation between pathogen growth and host transcriptional response.

Induction of an ocular inflammatory response. The cascade of cytokine expression and immune cell infiltration that follows HSV-1 infection of the cornea causes much of the damage observed in herpetic stromal keratitis (7, 9). Given the disease pathology of our infected mice and the clinical relevance of

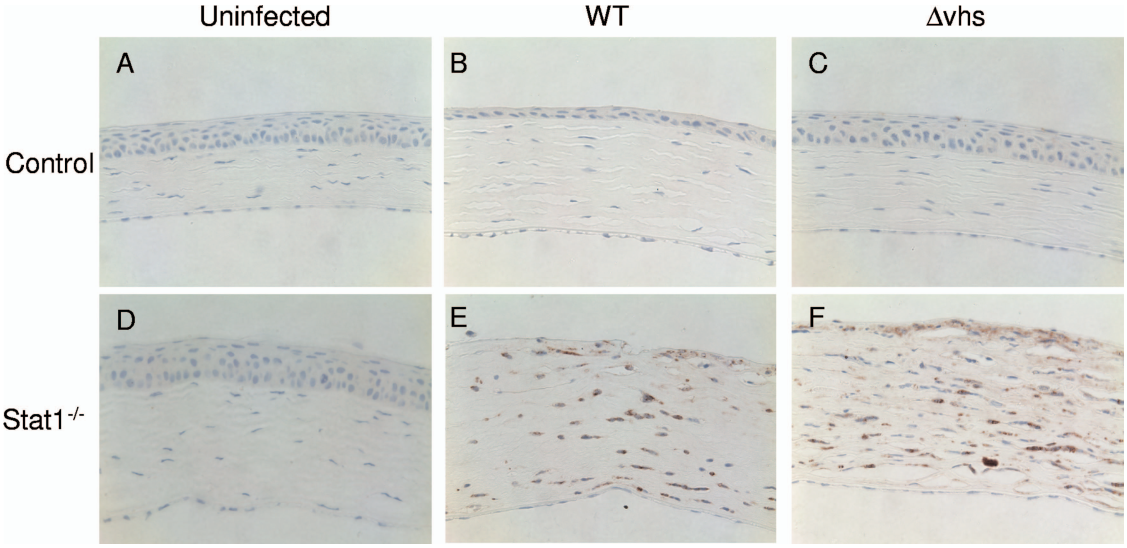

FIG. 3. Neutrophil infiltration of infected cornea. Corneas of control (A, B, and C) and Stat1$^{-/-}$ mice (D, E, and F) were scarified and mock treated (A and D) or inoculated with 2×10^6 PFU per eye of WT virus (B and E) or Δ*vhs* virus (C and F). Eyeballs harvested at 3 dpi were formalin fixed, sectioned, and then stained with hematoxylin and probed with anti-Ly6 and streptavidin-HRP. A representative image from four eyeballs studied is shown.

cytokine expression, we focused our search of the host genomics data to a list of inflammatory cytokines known to have a role in HSK development, in addition to ISGs downstream of IFN signaling. Gene expression changes were analyzed in a mouse-, virus-, and time-dependent manner (Table 1).

In all infected control mice, changes in expression of the genes implicated in inflammatory response were modest and transient, especially in the Δ*vhs* virus-infected mice. For the most part, immune gene expression correlated with viral replication, and this effect was most evident when comparing replication of both viruses to gene expression levels at 2 and 3 dpi.

In the infected Stat1$^{-/-}$ mice there was a substantial, yet delayed induction of inflammatory genes compared to the infected control mice. The increased transcriptional profiles correlated closely with the biological readout of disease score but did not completely correlate with viral replication. The Stat1$^{-/-}$ samples showed a sustained upregulation of immune

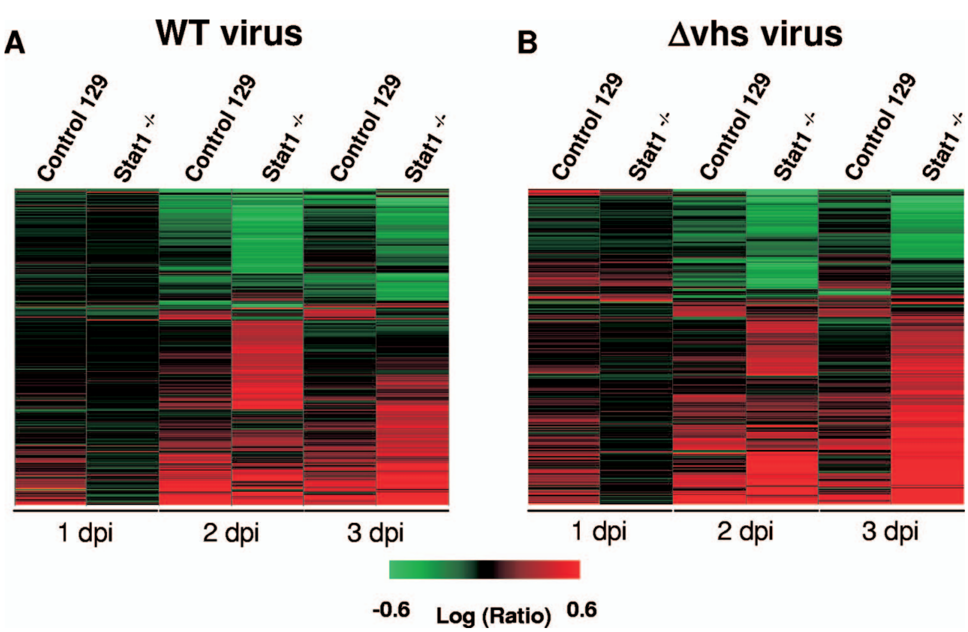

FIG. 4. Overview of changed genes following corneal infection. Total RNA was harvested from control or Stat1$^{-/-}$ mice infected with either WT virus (A) or Δ*vhs* virus (B) over a 3-day time course. Heat maps show the 3,278 genes changed at least ≥2-fold compared to mock-treated corneas ($P \leq 0.01$) in at least one of the two time point experiments being compared. Respectively, red, green, and black represent upregulated, downregulated, and unchanged compared to mock-treated corneas.

TABLE 1. Fold change of infected versus mock-infected corneas of selected inflammation-associated genes and ISGs

Gene	Description	Fold change[a] in gene expression											
		Control 129 mice						Stat1$^{-/-}$ mice					
		WT virus			Δvhs virus			WT virus			Δvhs virus		
		1 dpi	2 dpi	3 dpi	1 dpi	2 dpi	3 dpi	1 dpi	2 dpi	3 dpi	1 dpi	2 dpi	3 dpi
Acute-phase response proteins													
IL-1α	Interleukin-1α	*1.23*	3.47	2.28	*1.64*	*3.03*	*1.33*	*–1.12*	*1.54*	*1.94*	*1.04*	2.90	2.60
IL-1β	Interleukin-1β	4.20	5.36	4.74	5.47	*1.84*	*1.54*	*1.42*	**36.35**	**87.96**	*1.58*	**68.31**	**69.09**
IL-6	Interleukin-6	3.08	2.33	*1.30*	*1.05*	*1.19*	*–1.47*	*1.00*	**77.37**	**82.52**	*1.00*	**43.36**	**14.58**
TNF-α	Tumor necrosis factor alpha	*1.32*	*1.72*	*1.36*	*–1.09*	*1.26*	*1.32*	*1.20*	*2.10*	*1.97*	*1.17*	2.30	*1.76*
Chemokines													
CCL2	Chemokine (C-C motif) ligand 2; MCP-1	**11.03**	8.95	3.65	5.30	3.44	*1.80*	*1.81*	**12.69**	**16.78**	*1.66*	**15.89**	**12.93**
CCL3	Chemokine (C-C motif) ligand 3; MIP-1α	*1.68*	2.42	2.14	4.48	2.38	*1.55*	*1.21*	6.80	**27.74**	*1.50*	4.81	**24.16**
CCL4	Chemokine (C-C motif) ligand 4; MIP-1β	4.36	**10.01**	4.03	8.40	3.00	*1.35*	*1.02*	**16.08**	**94.21**	*–1.20*	**25.52**	**89.70**
CCL5	Chemokine (C-C motif) ligand 5; RANTES	2.54	**10.40**	3.52	*1.85*	4.64	*1.50*	*–1.58*	2.30	**17.74**	*–1.45*	4.47	**23.49**
CCL12	Chemokine (C-C motif) ligand 12; MCP-5	3.73	3.05	*1.01*	2.65	1.77	*–1.07*	*–1.36*	4.85	**15.52**	*1.00*	**10.77**	**15.48**
CXCL1	Chemokine (C-X-C motif) ligand 1; KC	*3.01*	*1.52*	*1.44*	*3.43*	*1.04*	*1.68*	*1.62*	**20.32**	**24.24**	*1.22*	**34.87**	6.35
CXCL2	Chemokine (C-X-C motif) ligand 2; MIP-2α	*1.11*	*1.32*	*–1.07*	*–1.37*	*1.13*	*1.64*	*1.07*	2.48	6.00	*1.11*	3.15	6.44
CXCL9	Chemokine (C-X-C motif) ligand 9	6.28	**39.75**	8.63	*2.22*	**18.02**	*2.85*	*1.00*	*–1.46*	8.72	*1.00*	*1.65*	6.76
CXCL10	Chemokine (C-X-C motif) ligand 10; IP-10	**65.08**	**53.83**	8.64	**40.54**	**10.00**	*2.76*	*1.00*	**78.95**	**571.37**	*1.00*	**187.94**	520.68
IFNs and ISGs													
IFN-α	Alpha interferon	*0.00*	*0.00*	*0.00*	*0.00*	*0.00*	*0.00*	*0.00*	*0.00*	2.03	*0.00*	**11.88**	2.11
IFN-β	Beta interferon	*1.54*	*1.73*	*–1.39*	*1.00*	*–1.01*	*–1.24*	*1.00*	5.31	**12.26**	*–1.08*	**13.47**	4.74
IFN-γ	Gamma interferon	2.41	8.17	*1.16*	*–1.15*	2.39	*1.14*	*–1.24*	6.70	5.60	*1.00*	**13.27**	**10.96**
IFIT1	IFN-induced protein with tetratricopeptide repeats 1	3.89	**10.14**	8.48	2.83	9.15	8.74	*–1.05*	5.12	**40.49**	*–1.01*	**10.64**	**47.12**
ISG15	ISG15 ubiquitinlike modifier; G1p2	2.09	6.14	8.21	*1.73*	6.44	*7.72*	*–1.07*	2.24	**14.42**	*–1.14*	4.47	**15.15**

[a] That is, the fold change compared to mock-infected corneas. Italicized numbers indicate genes that did not meet the criteria of being at least twofold changed compared to mock-infected corneas ($P \leq 0.01$). Boldface entries indicate genes that changed at least 10-fold compared to mock-infected corneas ($P \leq 0.01$).

response genes, regardless of the presence or absence of vhs. We also observed evidence of Stat1-independent IFN gene expression, including upregulation of ISG15 and IFIT1. While some ISGs are expressed in a Stat1-independent manner (13, 36, 37), the heightened expression in these mice was unexpected. That ISGs are strongly expressed, combined with the IFN sensitivity of Δ*vhs* viruses, together may in part explain the persistent attenuation of Δ*vhs* virus in Stat1$^{-/-}$ mice.

IPA of relevant pathways. To look beyond genes known to have a role in ocular pathology, we further characterized the types of genes that met our fold-change selection parameters, using IPA software. Five functional pathways that have roles in antiviral establishment and disease pathology were identified in which significant differences were observed when the profiles were compared in a virus-, mouse-, or time-dependent fashion (Fig. 5). Both vhs- and Stat1-dependent effects were observed in the pathways discussed in further detail below.

Many intracellular cascades are activated in response to TLR ligand binding, including NF-κB, IRF-3, and mitogen-activated protein kinase pathways (1, 6). IPA identified significant differences between the control and Stat1$^{-/-}$ mice in the TLR signaling pathway category of genes (Fig. 5 and see Table S1 in the supplemental material). In the control mice, only PKR (eIF2αk2) was consistently and substantially changed in response to infection, while all infected Stat1$^{-/-}$ mice demonstrated upregulation of the TLRs 2, 3, 6, and 7, as well as the transcriptional activators Fos and Jun.

Changes in IL-6 and IL-6 signaling-dependent genes were mostly Stat1 dependent (Fig. 5 and see Table S2 in the supplemental material). IL-6 and IL-1β, both involved in the acute-phase response, were upregulated at 2 and 3 dpi in the corneas of Stat1$^{-/-}$ mice. The IL-6 receptor can mediate transcriptional changes via Stat3, and numerous Stat3-dependent genes were strongly upregulated in a Stat1-dependent manner, a finding suggestive of increased IL-6 and Stat3 mediated signaling in the Stat1$^{-/-}$ mice. IL-6 has been strongly implicated in the genesis of HSK, and therefore it was notable that the Stat1$^{-/-}$ mice showed such elevated disease and pathology.

Apoptosis signaling genes were differentially regulated between our model systems (Fig. 5 and see Table S3 in the

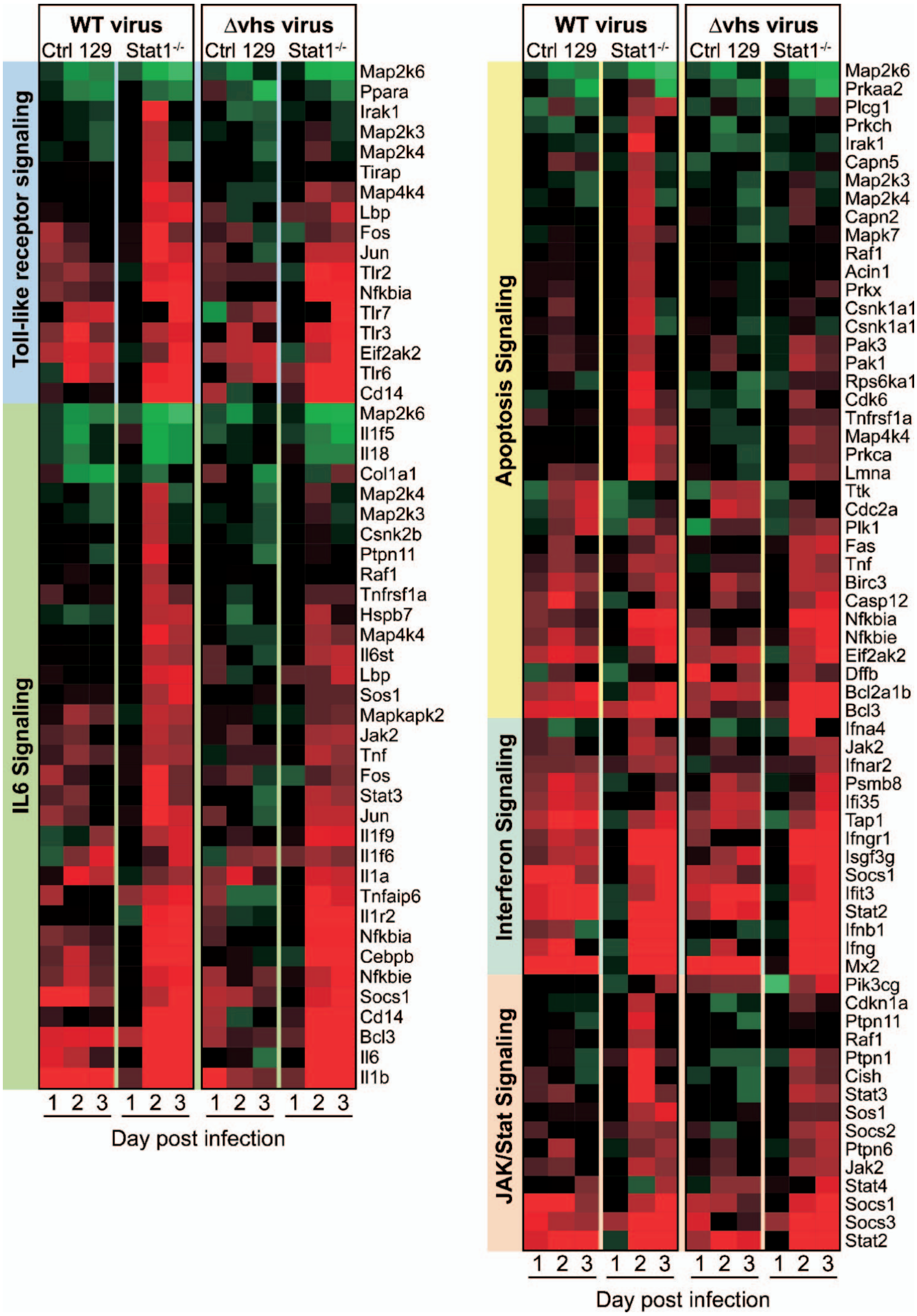

FIG. 5. Heap map of changed genes involved in selected immune responses. Heat maps were generated to show the relative expression levels of selected immune response genes that changed ≥2-fold compared to mock-treated corneas ($P \leq 0.01$). Changed genes (detailed on right side of maps) were bundled into their relevant category (detailed on left side of maps). The sample and time postinfection are listed at the top and bottom of the maps. Red, green, and black indicate that each gene is, respectively, upregulated, downregulated, or unchanged compared to a mock sample.

supplemental material). The genes from this category could be broadly sorted into two groups on the basis of expression pattern. The first group included genes that were upregulated at 2 dpi in the Stat1$^{-/-}$ mice, with the WT virus-infected Stat1$^{-/-}$ mice showing the most changes. The second group of genes was for the most part changed in all infection models, with the magnitude of change being greater in the Stat1$^{-/-}$ mice than in the control mice. This group of genes included caspase-12, PKR, Fas, Tnf, and NF-κB inhibitors (Nfkbia and Nfkbie). A small group of genes involved in DNA damage checkpoint pathway (Ttk, Cdc2a, and Plk1) were upregulated more strongly in the control mice. Interestingly, genes with

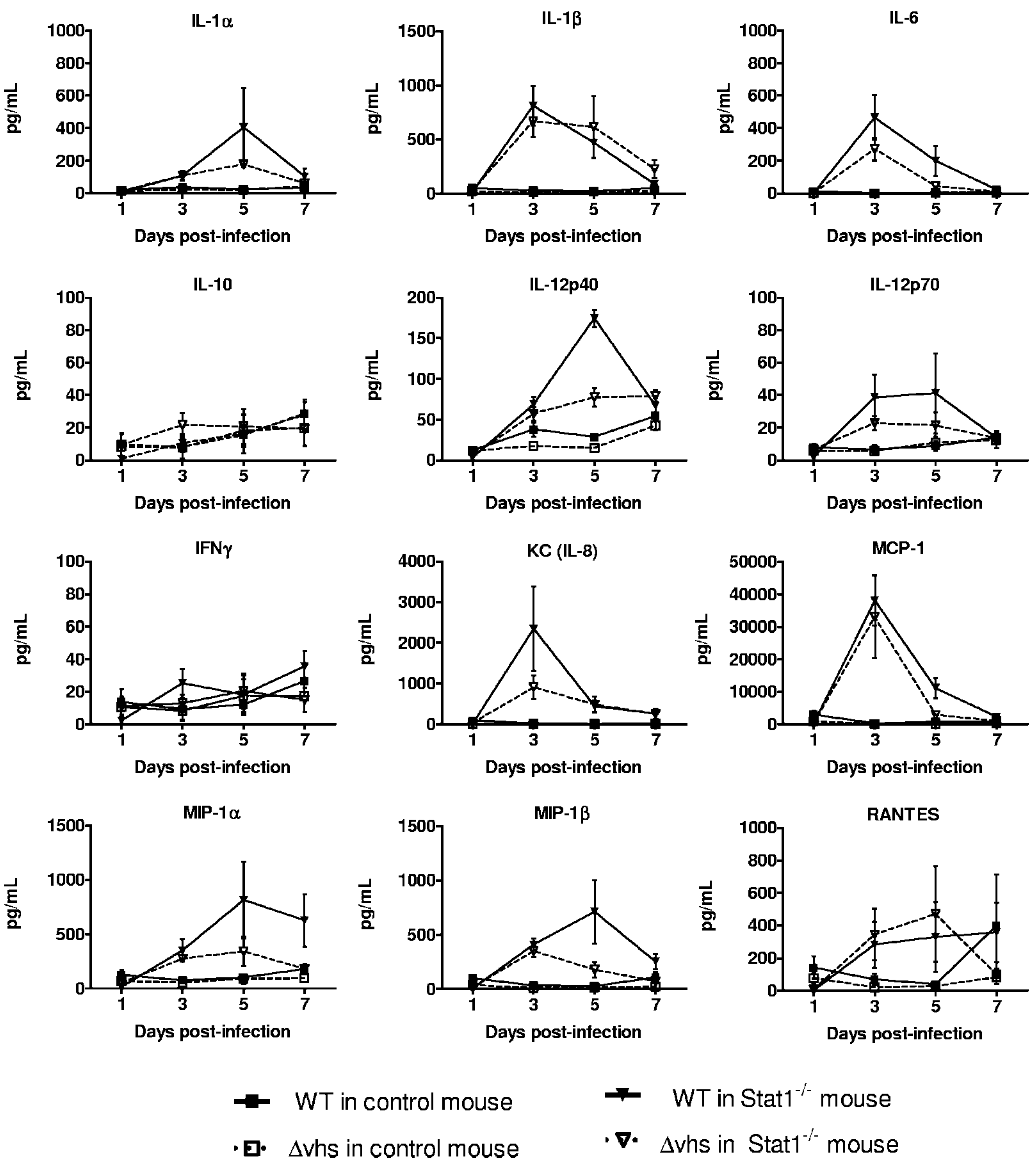

FIG. 6. Multiplex cytokine analysis of infected corneas. The corneas of control and Stat1$^{-/-}$ mice were scarified and mock treated or inoculated with 2×10^6 PFU per eye of WT or Δ*vhs* virus for 1, 3, 5, or 7 dpi. Cornea lysates were analyzed with a multiplex cytokine array. Average cytokine concentrations determined from at least four mice are reported as pg/ml (*y* axis). For clarity, mock samples were omitted from the graphs.

antiapoptotic functions were also identified (Birc3, Bcl2a1b, and Bcl3). The mechanism through which these genes are upregulated and how this gene expression program affects viral replication is unknown.

Both type I and type II IFN signal through their respective receptors to JAK/Tyk and STATs (reviewed in reference 45). The control and Stat1$^{-/-}$ mice showed similar levels of changed genes involved in the IFN signaling pathway, regardless of infecting virus (Fig. 5 and see Table S4 in the supplemental material). However, when JAK/Stat signaling genes were specifically examined, the Stat1$^{-/-}$ mice had greater changes in this group of genes, with WT virus-infected Stat1$^{-/-}$ corneas showing the greatest number of changed genes (Fig. 5 and see Table S5 in the supplemental material). Given the IFN sensitivity of Δ*vhs* viruses, this elevated ISG expression may explain why the Δ*vhs* virus remained attenuated in the Stat1$^{-/-}$ mice.

Cytokine production reflects strong induction of inflammatory response. To validate our genomics analysis and measure cytokine induction at the protein level, we harvested infected corneas for analysis with a Bio-Plex multiplex cytokine array designed to simultaneously analyze multiple mouse cytokines. We focused our attention to a select list of cytokines previously known to be factors in HSV-1 ocular pathogenesis. The data shown contain at least four mice per data point (Fig. 6). All mock-treated mice showed near-background levels of all cytokines tested (data not shown). In infected control mice, few cytokine changes were observed, and most changes were <10-fold compared to mock-treated samples. In contrast, the infected Stat1$^{-/-}$ corneas

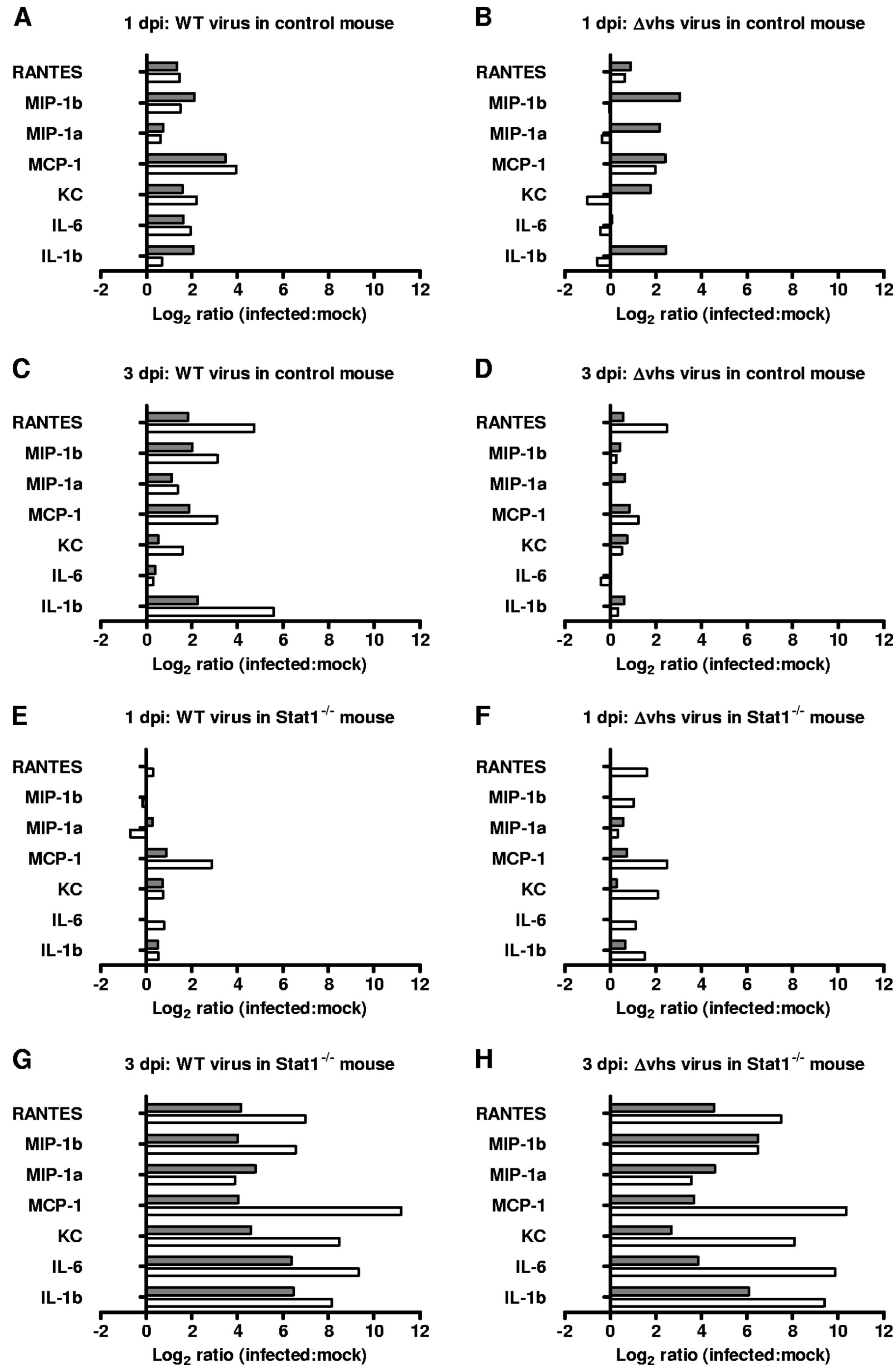

FIG. 7. Cytokine analysis correlates with genomics study. To directly compare the genomics study to the cytokine analysis, the fold change (infected versus mock) values were converted to $\log_2$ ratio and plotted with the genomics data. The mouse, virus, and time postinfection are indicated at the top of each graph. Gray and white bars represent gene array and cytokine data, respectively.

showed considerable changes in cytokine expression starting on 3 dpi. In general, the WT virus-infected Stat1$^{-/-}$ showed greater changes than the Δ*vhs*-infected mice, and the expression of most cytokines peaked on day 3 postinfection. Substantial cytokine expression changes were observed for IL-6, KC (IL-8), MCP-1, and RANTES, while more moderate changes were observed with IL-1α, IL-β, IL-12p40, MIP-1α, and MIP-1β. Changes in the expression of IL-10, IL-12p70, and IFN-γ were low.

To correlate these results to the genomics study, the fold change (infected versus mock) values for seven cytokines were converted to a $\log_2$ ratio and plotted in conjunction with the genomics data (Fig. 7; see Table S6 in the supplemental material). Because the arrays and cytokine analysis relied on dif-

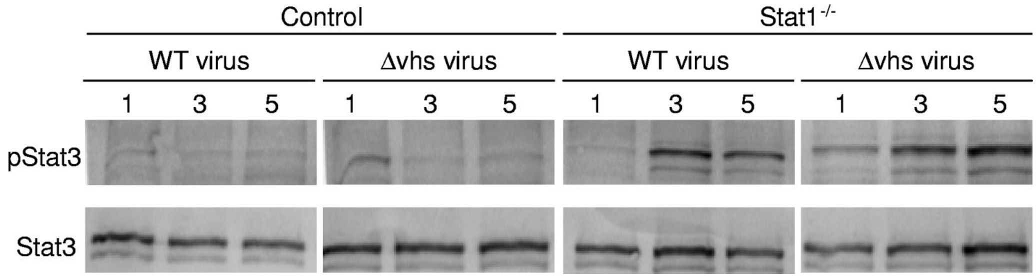

FIG. 8. Western blot analysis of Stat3 phosphorylation. Lysates generated from corneas of control and Stat1$^{-/-}$ mice infected with either WT virus or Δ*vhs* virus for 1, 3, and 5 dpi were probed for phosphorylated Stat3 (upper panels) and total Stat3 (lower panels) by Western blotting. At least three mice for each infection condition and time point were analyzed, and a representative blot is shown.

ferent methods (oligonucleotide and antibody binding, respectively), the absolute numbers should not be compared, but rather demonstrate the trends of expression. Overall, our cytokine expression analysis strongly correlated with our genomics study, in terms of the magnitude and time course of the cytokine expression changes. In particular, this presentation of the data highlights and validates the delay of cytokine expression in the Stat1$^{-/-}$ mice first observed in the genomics analysis (compare Fig. 7E and F to Fig. 7G and H). Again, we propose that this delay, likely due to aberrant immune signaling or activation of Stat1-independent pathways in the absence of Stat1, benefits the virus and allows for increased viral replication in these mice.

Stat3 is activated in the corneas of infected Stat1$^{-/-}$ mice. Thus, far we had demonstrated that the HSV-1-infected Stat1$^{-/-}$ mouse corneas experience significant changes in not only IL-6 expression (Table 1 and Fig. 6) but also in IL-6- and Stat3-dependent gene expression (Fig. 5). The heightened IL-6 expression was likely to be, at least in part, a causative agent of the cornea damage and neutrophil invasion reported above (Fig. 3). Other groups have reported that in the absence of Stat1, Stat3 experiences increased and prolonged activation of Stat3 in response to IL-6 and IFN-γ (15, 34, 38, 50). The IL-6 receptor can associate with and signal through Stat3 (2, 51), which upon activation dimerizes and translocates to the nucleus to mediate a gene expression pattern different from that of Stat1 (11, 41).

To address this further, we assayed for activation of Stat3 in infected corneas harvested at 1, 3, and 5 dpi, probing for total Stat3 and phosphorylated Stat3 (Y705) by Western blotting. The levels of total Stat3 remained similar throughout all samples (Fig. 8). All mock-treated samples showed minimal Stat3 phosphorylation (data not shown), and there was only a transient phosphorylation of Stat3 at 1 dpi in the infected control mice. In contrast, infected Stat1$^{-/-}$ corneas showed a prominent increase in Stat3 phosphorylation at 3 dpi. This heightened phosphorylation was evident out to at least 5 dpi in both WT virus- and Δ*vhs* virus-infected Stat1$^{-/-}$ mouse corneas.

To determine whether the positive Stat3 phosphorylation signal derived from resident cornea cells and/or infiltrating cells, we also examined Stat3 phosphorylation via immunohistochemistry at 3 dpi (Fig. 9). The mock-treated and all control mice showed minimal Stat3 phosphorylation (Fig. 9A to D). As expected, the infected Stat1$^{-/-}$ mice corneas were positive for

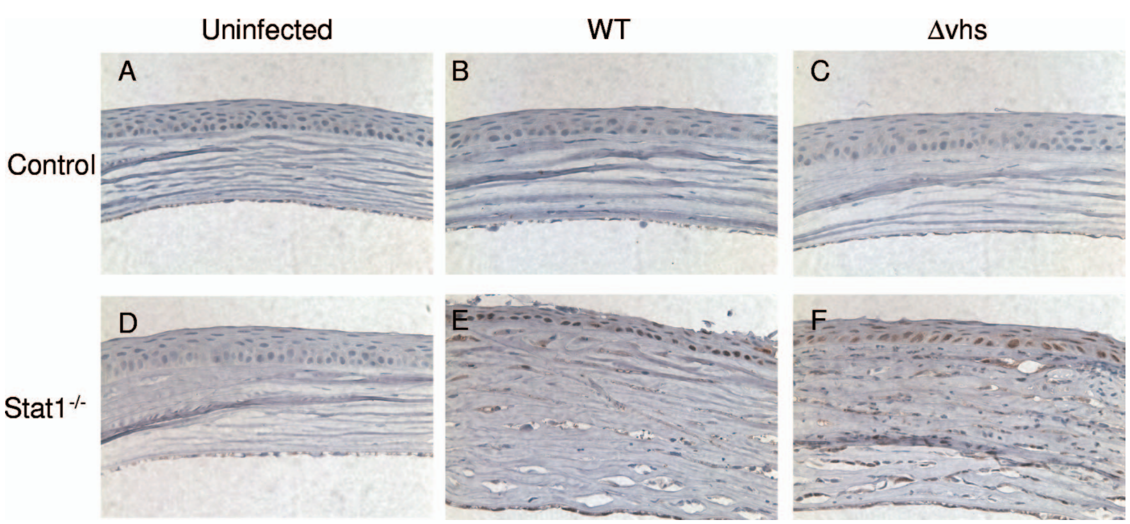

FIG. 9. Immunohistochemistry analysis of Stat3 phosphorylation. Corneas of control (A, C, and E) and Stat1$^{-/-}$ (D, E, and F) mice were scarified and mock treated (A and D) or inoculated with 2×10^6 PFU per eye of WT (B and E) or Δ*vhs* virus (C and F). Eyeballs harvested at 3 dpi were formalin fixed, sectioned, and then stained with hematoxylin and probed for phosphorylated Stat3 with streptavidin-HRP. A representative image from four eyeballs studied is shown.

phosphorylated Stat3, and this signal was localized to the nuclei of the cornea epithelium, the outermost cell layer in the cornea (Fig. 9E and F).

Taken together, our data show sustained activation of Stat3 in the absence of Stat1. This activation of Stat3 directly correlates with increased neutrophil invasion, disease pathology, IL-6-dependent gene expression, and increased expression of inflammatory mediators. As such, we theorize that many of the gene expression changes and pathologies found in the Stat1$^{-/-}$ mice results from aberrant Stat3 activation.

DISCUSSION

In this study, we have demonstrated that HSV-1 vhs and Stat1 play pivotal roles in the control of host gene expression and disease pathology. vhs was important for viral replication, even in highly susceptible Stat1$^{-/-}$ mice, since the Δ*vhs* virus showed reduced titers in all tissues tested, and the Stat1$^{-/-}$ mice were able to survive the infection. Stat1 was also important for controlling the timing and amplitude of the inflammatory response. Although it was notable that both WT and Δ*vhs* virus replication was increased in the Stat1$^{-/-}$ mice, it was of particular interest that viral replication and disease did not completely correlate. Specifically, there was a high level of inflammation in the corneas of Δ*vhs* virus-infected Stat1$^{-/-}$ mice, and no apparent inflammation in WT virus-infected control mice, yet each had similar virus titers. This finding, therefore, contradicts the general assumption that host gene expression and disease correlate closely with the level of viral replication.

Our studies confirm a role for vhs in replication, but not for control of host inflammatory pathways. We had initially theorized that the attenuation of Δ*vhs*, in both the control and Stat1$^{-/-}$ mice, was due to heightened host response, and yet our current studies revealed few indications of a hyperactivated immune response in the absence of vhs. Although the replication of Δ*vhs* virus is enhanced in the Stat1$^{-/-}$ mice, it was not equivalent to that of the WT virus. Its continued attenuation might be attributed to redundant Stat1-independent IFN gene expression pathways identified in these mice, coupled with the heightened susceptibility of vhs-null viruses to IFN. These data call into question, however, the supposition that Δ*vhs* virus gets cleared rapidly due to its inability to shut off IFN-stimulated gene expression.

In addition, the persistent attenuation of Δ*vhs* virus could stem from the fact that this virus appears to have an inherent defect in replication that cannot be compensated for by deletion of a host factor. This idea is supported by the fact that even when inoculated into Stat1$^{-/-}$ or IFNαβγR$^{-/-}$ mice the Δ*vhs* virus was still attenuated. Furthermore, in vitro, Δ*vhs* virus is still growth impaired relative to WT virus (~10-fold) in IFNαβγR$^{-/-}$ MEFs (32). Whether this defect is due to the loss of vhs RNase activity or another role for vhs remains to be determined. Indeed, alterations in the gE/gI complex have been shown in viruses lacking vhs, possibly explaining this IFN-independent growth deficit (18).

The infected Stat1$^{-/-}$ mice showed disease progression that was not correlated to viral growth. The clouded corneas and ocular discharge observed by 2 dpi, however, correlated with an increase in neutrophil invasion and cytokine expression. Both genomics and cytokine analyses identified IL-6- and IL-6-dependent gene expression as different between the two mouse strains. HSV-1-infected IL-6$^{-/-}$ mice showed a role for IL-6 in inducing ocular pathology, chemokine expression, and cellular invasion (12). These studies support our hypothesis that the strong proinflammatory IL-6 signaling observed in our Stat1$^{-/-}$ mice is a likely source of the severe ocular disease and neutrophil infiltration. HSV-1-infected IL-6$^{-/-}$ mice, however, showed mortality, ocular shedding, and neuronal spread similar to that of IL-6$^{+/+}$ mice (22). This lack of antiviral activity mediated by IL-6 may in part explain why the Stat1$^{-/-}$ mice are still unable to control HSV-1 infection despite significantly enhanced immune gene expression.

The idea that IL-6 mediates disease progression is supported by our finding that HSV-1 Stat1$^{-/-}$ mice showed heightened phosphorylation of Stat3, a transcription factor that is activated in response to IL-6 and IFN-γ receptor interactions (15, 34, 38). The low levels of IFN-γ observed in our early time course suggest that IL-6 is the more likely mediator of Stat3 activation in our system. Previous studies have documented heightened and prolonged activation of Stat3 in the absence of Stat1 (15, 34, 38). From this, we hypothesize that the heightened activation of Stat3 induces a pattern of gene expression in Stat1$^{-/-}$ mice not observed in the controls. IL-6 is a Stat3-dependent gene, so it is likely that IL-6-dependent Stat3 activation initiates a positive feedback, thereby inducing further IL-6 expression, which in turn enhances the inflammatory response and disease progression. The inflammatory process found in some chronic inflammatory diseases has been linked to gene expression patterns dependent on IL-6 activation of Stat3 (4, 5). Suppressor of cytokine signaling 1 and 3 (SOCS1 and SOCS3) are IFN-dependent genes known to serve as negative feedback regulators of Stat1 and Stat3, respectively. Our genomics analysis found upregulation of SOCS1 and SOCS3 expression at 1 dpi in the control mice had tapered down by 3 dpi, reflecting a normal signaling process. SOCS3 upregulation, which was greater in Stat1$^{-/-}$ mice than in control mice, was not observed until 2 to 3 dpi in these mice. This delay, concordant with the delay observed in other immune response genes in these mice, may contribute to the deregulation of cytokine signaling. Consistent with this idea, mice lacking SOCS3 show delayed wound healing and prolonged inflammation (52).

In Stat1$^{-/-}$ mice, both WT and Δ*vhs* viruses showed more productive replication at the cornea, more so than previously observed with IFNαβγR$^{-/-}$ mice (24). This was in contrast to studies that showed Stat1$^{-/-}$ mice are more resistant to Sindbis virus and MCMV infection than IFNαβγR$^{-/-}$ mice (13). Given the existence of Stat1-independent signaling it is not unexpected that Stat1$^{-/-}$ and IFNαβγR$^{-/-}$ mice differ in susceptibility to virus infection. The contrasting susceptibilities to HSV, Sindbis virus, and MCMV likely reflect either the efficiency with which the Stat1-independent signaling pathways can protect against specific pathogens or, alternatively, the differential abilities of these pathogens to subvert the Stat1 independent pathways. Interactions between the type I IFN receptor and IL-6 signaling, as well as the presence of Stat1 to balance Stat3 signaling, may in part account for the differences observed between HSV-1-infected Stat1$^{-/-}$ and IFNαβγR$^{-/-}$ mice (28).

A number of previous studies have demonstrated enhancement or restoration of growth and virulence of attenuated viruses in immunodeficient mice (14, 24, 25). We found that although the growth of the Δ*vhs* virus was restored in the $Stat1^{-/-}$ mice, comparable to the WT virus in the control mouse, the gene expression patterns and disease pathologies of these infection models were not similar. An important point of the present study is that the enhancement of virulence is not necessarily paralleled by comparably altered gene expression patterns. This stresses the need for caution when interpreting data in which virulence or the growth of attenuated viruses is restored in immunodeficient mice. Moreover, there was scant evidence from the array data to support the idea that Δ*vhs* was cleared in the control mice due to heightened IFN-driven antiviral activity. Nevertheless, our data show the importance of vhs for promoting viral replication in the presence of the innate immune response, and the importance of Stat1 in limiting virus infection and for facilitating an appropriate nonpathological inflammatory response. The outcome of HSV infection is therefore determined by a delicate balance between viral immunomodulators and host response pathways. A better understanding of this interaction may lead to improved understanding and therapeutics for treating HSV diseases, many of which are immunopathological in nature.

In addition, the survival of even highly immunocompromised mice following infection with high doses of Δ*vhs* provides further impetus for the idea that viruses lacking vhs in combination with the deletion of other virulence genes may offer both improved safety and efficacy as live-attenuated vaccines.

ACKNOWLEDGMENTS

This study was supported by National Institutes of Health grants to D.A.L. (EY10707 and EY09083), to T.J.P. (1F32 AI65069-01A2), to M.G.K. (P30 DA015625), and to the Department of Ophthalmology and Visual Sciences (P30EY02687). Support for the Department from Research to Prevent Blindness and a Lew Wasserman Scholarship to D.A.L. are gratefully acknowledged.

We thank Belinda McMahon for assistance with histology and Tracey Baas for assistance with the analysis of the gene expression data.

REFERENCES

1. **Aderem, A., and R. J. Ulevitch.** 2000. Toll-like receptors in the induction of the innate immune response. Nature **406:**782–787.
2. **Akira, S., Y. Nishio, M. Inoue, X. J. Wang, S. Wei, T. Matsusaka, K. Yoshida, T. Sudo, M. Naruto, and T. Kishimoto.** 1994. Molecular cloning of APRF, a novel IFN-stimulated gene factor 3 p91-related transcription factor involved in the gp130-mediated signaling pathway. Cell **77:**63–71.
3. **Araki-Sasaki, K., T. Tanaka, Y. Ebisuno, H. Kanda, E. Umemoto, K. Hayashi, and M. Miyasaka.** 2006. Dynamic expression of chemokines and the infiltration of inflammatory cells in the HSV-infected cornea and its associated tissues. Ocul. Immunol. Inflamm. **14:**257–266.
4. **Atreya, R., and M. F. Neurath.** 2008. Signaling molecules: the pathogenic role of the IL-6/STAT-3 trans signaling pathway in intestinal inflammation and in colonic cancer. Curr. Drug Targets **9:**369–374.
5. **Carey, R., I. Jurickova, E. Ballard, E. Bonkowski, X. Han, H. Xu, and L. A. Denson.** 2008. Activation of an IL-6:STAT3-dependent transcriptome in pediatric-onset inflammatory bowel disease. Inflamm. Bowel Dis. **14:**446–457.
6. **Carmody, R. J., and Y. H. Chen.** 2007. Nuclear factor-κB: activation and regulation during Toll-like receptor signaling. Cell Mol. Immunol. **4:**31–41.
7. **Carr, D. J., and L. Tomanek.** 2006. Herpes simplex virus and the chemokines that mediate the inflammation. Curr. Top. Microbiol. Immunol. **303:**47–65.
8. **Chomczynski, P., and N. Sacchi.** 1987. Single-step method of RNA isolation by acid guanidinium thiocyanate-phenol-chloroform extraction. Anal. Biochem. **162:**156–159.
9. **Deshpande, S. P., M. Zheng, S. Lee, and B. T. Rouse.** 2002. Mechanisms of pathogenesis in herpetic immunoinflammatory ocular lesions. Vet. Microbiol. **86:**17–26.
10. **Dupuis, S., E. Jouanguy, S. Al-Hajjar, C. Fieschi, I. Z. Al-Mohsen, S. Al-Jumaah, K. Yang, A. Chapgier, C. Eidenschenk, P. Eid, A. Al Ghonaium, H. Tufenkeji, H. Frayha, S. Al-Gazlan, H. Al-Rayes, R. D. Schreiber, I. Gresser, and J. L. Casanova.** 2003. Impaired response to interferon-alpha/beta and lethal viral disease in human STAT1 deficiency. Nat. Genet. **33:**388–391.
11. **Ehret, G. B., P. Reichenbach, U. Schindler, C. M. Horvath, S. Fritz, M. Nabholz, and P. Bucher.** 2001. DNA binding specificity of different STAT proteins: comparison of in vitro specificity with natural target sites. J. Biol. Chem. **276:**6675–6688.
12. **Fenton, R. R., S. Molesworth-Kenyon, J. E. Oakes, and R. N. Lausch.** 2002. Linkage of IL-6 with neutrophil chemoattractant expression in virus-induced ocular inflammation. Investig. Ophthalmol. Vis. Sci. **43:**737–743.
13. **Gil, M. P., E. Bohn, A. K. O'Guin, C. V. Ramana, B. Levine, G. R. Stark, H. W. Virgin, and R. D. Schreiber.** 2001. Biologic consequences of Stat1-independent IFN signaling. Proc. Natl. Acad. Sci. USA **98:**6680–6685.
14. **Halford, W. P., C. Weisend, J. Grace, M. Soboleski, D. J. Carr, J. W. Balliet, Y. Imai, T. P. Margolis, and B. M. Gebhardt.** 2006. ICP0 antagonizes Stat 1-dependent repression of herpes simplex virus: implications for the regulation of viral latency. Virol. J. **3:**44.
15. **Hong, F., B. Jaruga, W. H. Kim, S. Radaeva, O. N. El-Assal, Z. Tian, V. A. Nguyen, and B. Gao.** 2002. Opposing roles of STAT1 and STAT3 in T cell-mediated hepatitis: regulation by SOCS. J. Clin. Investig. **110:**1503–1513.
16. **Johnson, A. C., F. P. Heinzel, E. Diaconu, Y. Sun, A. G. Hise, D. Golenbock, J. H. Lass, and E. Pearlman.** 2005. Activation of Toll-like receptor (TLR)2, TLR4, and TLR9 in the mammalian cornea induces MyD88-dependent corneal inflammation. Investig. Ophthalmol Vis Sci. **46:**589–595.
17. **Jouanguy, E., S. Y. Zhang, A. Chapgier, V. Sancho-Shimizu, A. Puel, C. Picard, S. Boisson-Dupuis, L. Abel, and J. L. Casanova.** 2007. Human primary immunodeficiencies of type I interferons. Biochimie **89:**878–883.
18. **Kalamvoki, M., J. Qu, and B. Roizman.** 2008. Translocation and colocalization of ICP4 and ICP0 in cells infected with herpes simplex virus 1 mutants lacking glycoprotein E, glycoprotein I, or the virion host shutoff product of the UL41 gene. J. Virol. **82:**1701–1713.
19. **Keadle, T. L., K. A. Laycock, J. L. Morris, D. A. Leib, L. A. Morrison, J. S. Pepose, and P. M. Stuart.** 2002. Therapeutic vaccination with vhs(−) herpes simplex virus reduces the severity of recurrent herpetic stromal keratitis in mice. J. Gen. Virol. **83:**2361–2365.
20. **Kurt-Jones, E. A., M. Chan, S. Zhou, J. Wang, G. Reed, R. Bronson, M. M. Arnold, D. M. Knipe, and R. W. Finberg.** 2004. Herpes simplex virus 1 interaction with Toll-like receptor 2 contributes to lethal encephalitis. Proc. Natl. Acad. Sci. USA **101:**1315–1320.
21. **Kwong, A. D., and N. Frenkel.** 1987. Herpes simplex virus-infected cells contain a function(s) that destabilizes both host and viral mRNAs. Proc. Natl. Acad. Sci. USA **84:**1926–1930.
22. **LeBlanc, R. A., L. Pesnicak, E. S. Cabral, M. Godleski, and S. E. Straus.** 1999. Lack of interleukin-6 (IL-6) enhances susceptibility to infection but does not alter latency or reactivation of herpes simplex virus type 1 in IL-6 knockout mice. J. Virol. **73:**8145–8151.
23. **Leib, D. A.** 2002. Counteraction of interferon-induced antiviral responses by herpes simplex viruses. Curr. Top. Microbiol. Immunol. **269:**171–185.
24. **Leib, D. A., T. E. Harrison, K. M. Laslo, M. A. Machalek, N. J. Moorman, and H. W. Virgin.** 1999. Interferons regulate the phenotype of wild-type and mutant herpes simplex viruses in vivo. J. Exp. Med. **189:**663–672.
25. **Lubinski, J., L. Wang, D. Mastellos, A. Sahu, J. D. Lambris, and H. M. Friedman.** 1999. In vivo role of complement-interacting domains of herpes simplex virus type 1 glycoprotein gC. J. Exp. Med. **190:**1637–1646.
26. **Lund, J., A. Sato, S. Akira, R. Medzhitov, and A. Iwasaki.** 2003. Toll-like receptor 9-mediated recognition of herpes simplex virus-2 by plasmacytoid dendritic cells. J. Exp. Med. **198:**513–520.
27. **Meraz, M. A., J. M. White, K. C. Sheehan, E. A. Bach, S. J. Rodig, A. S. Dighe, D. H. Kaplan, J. K. Riley, A. C. Greenlund, D. Campbell, K. Carver-Moore, R. N. DuBois, R. Clark, M. Aguet, and R. D. Schreiber.** 1996. Targeted disruption of the Stat1 gene in mice reveals unexpected physiologic specificity in the JAK-STAT signaling pathway. Cell **84:**431–442.
28. **Mitani, Y., A. Takaoka, S. H. Kim, Y. Kato, T. Yokochi, N. Tanaka, and T. Taniguchi.** 2001. Cross talk of the interferon-alpha/beta signalling complex with gp130 for effective interleukin-6 signalling. Genes Cells **6:**631–640.
29. **Morrison, L. A., and D. M. Knipe.** 1994. Immunization with replication-defective mutants of herpes simplex virus type 1: sites of immune intervention in pathogenesis of challenge virus infection. J. Virol. **68:**689–696.
30. **Murphy, J. A., R. J. Duerst, T. J. Smith, and L. A. Morrison.** 2003. Herpes simplex virus type 2 virion host shutoff protein regulates alpha/beta interferon but not adaptive immune responses during primary infection in vivo. J. Virol. **77:**9337–9345.
31. **Pasieka, T. J., T. Baas, V. S. Carter, S. C. Proll, M. G. Katze, and D. A. Leib.** 2006. Functional genomic analysis of herpes simplex virus type 1 counteraction of the host innate response. J. Virol. **80:**7600–7612.
32. **Pasieka, T. J., B. Lu, S. D. Crosby, K. M. Wylie, L. A. Morrison, D. E. Alexander, V. D. Menachery, and D. A. Leib.** 2008. Herpes simplex virus

virion host shutoff attenuates establishment of the antiviral state. J. Virol. **82:**5527–5535.
33. **Pasieka, T. J., B. Lu, and D. A. Leib.** 2008. Enhanced pathogenesis of an attenuated herpes simplex virus for mice lacking Stat1. J. Virol. **82:**6052–6055.
34. **Qing, Y., and G. R. Stark.** 2004. Alternative activation of STAT1 and STAT3 in response to interferon-gamma. J. Biol. Chem. **279:**41679–41685.
35. **Rader, K. A., C. E. Ackland-Berglund, J. K. Miller, J. S. Pepose, and D. A. Leib.** 1993. In vivo characterization of site-directed mutations in the promoter of the herpes simplex virus type 1 latency-associated transcripts. J. Gen. Virol. **74**(Pt. 9):1859–1869.
36. **Ramana, C. V., M. P. Gil, Y. Han, R. M. Ransohoff, R. D. Schreiber, and G. R. Stark.** 2001. Stat1-independent regulation of gene expression in response to IFN-gamma. Proc. Natl. Acad. Sci. USA **98:**6674–6679.
37. **Ramana, C. V., M. P. Gil, R. D. Schreiber, and G. R. Stark.** 2002. Stat1-dependent and -independent pathways in IFN-gamma-dependent signaling. Trends Immunol. **23:**96–101.
38. **Ramana, C. V., A. Kumar, and R. Enelow.** 2005. Stat1-independent induction of SOCS-3 by interferon-gamma is mediated by sustained activation of Stat3 in mouse embryonic fibroblasts. Biochem. Biophys. Res. Commun. **327:**727–733.
39. **Randall, R. E., and S. Goodbourn.** 2008. Interferons and viruses: an interplay between induction, signalling, antiviral responses and virus countermeasures. J. Gen. Virol. **89:**1–47.
40. **Sarangi, P. P., B. Kim, E. Kurt-Jones, and B. T. Rouse.** 2007. Innate recognition network driving herpes simplex virus-induced corneal immunopathology: role of the toll pathway in early inflammatory events in stromal keratitis. J. Virol. **81:**11128–11138.
41. **Seidel, H. M., L. H. Milocco, P. Lamb, J. E. Darnell, Jr., R. B. Stein, and J. Rosen.** 1995. Spacing of palindromic half sites as a determinant of selective STAT (signal transducers and activators of transcription) DNA binding and transcriptional activity. Proc. Natl. Acad. Sci. USA **92:**3041–3045.
42. **Smith, K. O.** 1964. Relationship between the envelope and the infectivity of herpes simplex virus. Proc. Soc. Exp. Biol. Med. **115:**814–816.
42a. **Stoughton, R., and H. Dai.** February 2002. Statistical combining of cell expression profiles. U.S. patent 6,351,712.
43. **Strelow, L. I., and D. A. Leib.** 1995. Role of the virion host shutoff (vhs) of herpes simplex virus type 1 in latency and pathogenesis. J. Virol. **69:**6779–6786.
44. **Suzutani, T., M. Nagamine, T. Shibaki, M. Ogasawara, I. Yoshida, T. Daikoku, Y. Nishiyama, and M. Azuma.** 2000. The role of the UL41 gene of herpes simplex virus type 1 in evasion of nonspecific host defense mechanisms during primary infection. J. Gen. Virol. **81:**1763–1771.
45. **Takaoka, A., and H. Yanai.** 2006. Interferon signalling network in innate defense. Cell Microbiol. **8:**907–922.
46. **Thomas, J., S. Gangappa, S. Kanangat, and B. T. Rouse.** 1997. On the essential involvement of neutrophils in the immunopathologic disease: herpetic stromal keratitis. J. Immunol. **158:**1383–1391.
47. **Toma, H. S., A. T. Murina, R. G. Areaux, Jr., D. M. Neumann, P. S. Bhattacharjee, T. P. Foster, H. E. Kaufman, and J. M. Hill.** 2008. Ocular HSV-1 latency, reactivation and recurrent disease. Semin. Ophthalmol. **23:**249–273.
48. **Walker, J., K. A. Laycock, J. S. Pepose, and D. A. Leib.** 1998. Postexposure vaccination with a virion host shutoff defective mutant reduces UV-B radiation-induced ocular herpes simplex virus shedding in mice. Vaccine **16:**6–8.
49. **Walker, J., and D. A. Leib.** 1998. Protection from primary infection and establishment of latency by vaccination with a herpes simplex virus type 1 recombinant deficient in the virion host shutoff (vhs) function. Vaccine **16:**1–5.
50. **Walters, D. M., A. Antao-Menezes, J. L. Ingram, A. B. Rice, A. Nyska, Y. Tani, S. R. Kleeberger, and J. C. Bonner.** 2005. Susceptibility of signal transducer and activator of transcription-1-deficient mice to pulmonary fibrogenesis. Am. J. Pathol. **167:**1221–1229.
51. **Zhong, Z., Z. Wen, and J. E. Darnell, Jr.** 1994. Stat3: a STAT family member activated by tyrosine phosphorylation in response to epidermal growth factor and interleukin-6. Science **264**:95–98.
52. **Zhu, B. M., Y. Ishida, G. W. Robinson, M. Pacher-Zavisin, A. Yoshimura, P. M. Murphy, and L. Hennighausen.** 2008. SOCS3 negatively regulates the gp130-STAT3 pathway in mouse skin wound healing. J. Investig. Dermatol. **128:**1821–1829.